Title: Methodological approaches to derive the heartbeat evoked potential: past practices and future recommendations.

Authors: Rania-Iman Virjee[1], Dr. Rohan Kandasamy[1,2,3], Prof. Sarah N Garfinkel[1], Prof. David Carmichael[4,5], Dr. Mahinda Yogarajah[2,3,6]

Affiliations: [1]Institute of Cognitive Neuroscience, University College London, [2]The department of Clinical Neurophysiology, The National Hospital for Neurology and Neurosurgery, [3]The Queen Square Institute of Neurology, UCL, [4]School of Biomedical Engineering and Imaging Sciences, King's College London, St. Thomas' Hospital, [5]Developmental Imaging and Biophysics, UCL Institute of Child Health, University College London, [6]The Epilepsy Society

Corresponding author information: Rania-Iman Virjee, rania-iman.virjee.18@ucl.ac.uk

Abstract

The heartbeat-evoked potential (HEP), a cortical response time-locked to each heartbeat, is suggested as an implicit electrophysiological marker reflecting the cortical processing of heartbeats, and more broadly interoceptive processing. An increasing number of studies suggest that HEP may be a meaningful clinical measure. However, on the scalp, HEP are low amplitude signals that are mixed with direct cardiac field artefacts. Therefore, signal processing pipelines that separate the cortical HEP from cardiac field artefacts are required. With a view to establishing optimal and standardised HEP pipelines, this review aims to evaluate the current approaches to this analysis used within the literature, address gaps and inconsistencies in HEP pipelines, and highlight the impact of crucial parameter choices. To do this, a scoping review investigated current HEP processing methods and parameters used in EEG and MEG studies. Testing these processing methods on Temple University's normal scalp EEG data (Obeid and Picone, 2016), the effect of different methods/parameters (e.g. HEP window, electrodes, filters, independent component analysis (ICA) and artefact subspace reconstruction (ASR)) on HEP extraction was explored.

EEG studies (N=101) demonstrated greater parameter variability and heterogeneity than MEG studies (N=10), although significantly more studies used EEG. ICA without cardiac field artefact and ASR at threshold 20 exhibit similar results for artefact removal. Statistical analysis revealed that the RR interval, the start and end of the HEP window and the start of the baseline correction window significantly affect HEP values in pre-frontal, frontal and centrotemporal electrodes.

Publications should report critical values for reliable HEP extraction, emphasising the need for standardised methods to enhance study comparison and reproducibility and establish a gold standard in the field.

Keywords: heartbeat evoked potential (HEP), electroencephalogram (EEG), magnetoencephalogram (MEG), methodological approaches, signal processing pipeline, interoception.

1. Introduction

Interoception is the process by which the nervous system senses, interprets, and integrates signals originating from within the body (e.g. hunger, thirst, cardiac and respiratory signals), providing a moment-by-moment mapping of the body's internal landscape across conscious and unconscious levels (Khalsa et al., 2018). This is essential for homeostasis and allostasis. Indeed, the heart continuously and cyclically communicates with the brain, impacting cognitive and emotional processes (Park and Blanke, 2019). First investigated by Schandry et al. (1986) and Jones et al. (1986), the heartbeat-evoked potential (HEP) is a cortical brain response that is time-locked to each heartbeat, which has been suggested as an implicit, electrophysiological marker reflecting the cortical processing of heartbeats (Kumral et al., 2022), and more broadly interoception. Since these initial publications in the early 1980s, HEP has gradually gained more attention in the literature, with publications rising to approximately 90 in the year 2021 (Shamsaei et al., 2010).

HEP appears to be a meaningful clinical measure. For example, HEP has been shown to have trait variation between groups such as in the ageing population (Kamp et al., 2021), and in groups with psychiatric conditions characterised by emotion dysregulation, including borderline personality disorder (BPD) (Flashbeck et al., 2020), and generalised anxiety disorder (GAD) (Pang et al., 2019; Schmitz et al., 2021). Other studies have shown state differences in HEP, including relationships with interoceptive processing (Baranauskas, Grabauskaitė and Griškova-Bulanova, 2017), as well as in the periods preceding functional seizures (FS) (Elkommos et al., 2023). Other studies aiming to validate brain stimulation techniques to interfere with interoceptive processes (Pollatos et al., 2016) and novel behavioural tasks to assess interoceptive processing in infants (Maister et al., 2017) have also utilised HEP.

Despite these promising earlier indicators of HEP utility, a fundamental inherent constraint is its susceptibility to contamination from direct electrical potential and associated magnetic flux when measuring it with electroencephalogram (EEG) or magnetoencephalography (MEG). This contamination arises from the electrophysiological activity of the heart which generates an electric field (i.e. the cardiac field artefact - CFA) that spreads throughout the whole body including the scalp (Arnau et al., 2023). Consequently, removing the CFA from HEP presents a significant challenge. This challenge stems from the limited capability to precisely measure the cardiac field and the incomplete understanding of its propagation towards the scalp (Yuan et al., 2007).

Studies have suggested various physiological sources underlying HEP (Park and Blanke, 2019). Previous work suggests that the physiological pathways are multifaceted and complex. HEP components can be noted in multiple cortical regions and temporal intervals, which may relate to distinct afferent signals from the carotid arteries and baroreceptors at the aortic arch (Gray et al., 2007; Garfinkel and Critchley, 2016), the cardiac afferent neurons (Tahsili-Fahadan and Geocadin, 2017), somatosensory pathways (Khalsa et al., 2009; Kern et al., 2013) and cortical neuro-vascular coupling (Kim et al., 2016). To date, studies have reported HEP in numerous sensor locations: frontal (Canales-Johnson et al., 2015; Babo-Rebelo et al., 2016a), central (Montoya et al., 1993; Petzschner et al., 2019) and parietal channels (Babo-Rebelo et al., 2016a; Pollatos and Schandry 2004; Kern et al. 2013). This variability in HEP topography is

thought to be generated by various methodological considerations and the widespread distribution of interoceptive processing in the brain including the insula, cingulate cortex, somatosensory cortex and amygdala. Variation in experimental design, such as the positioning of the reference, the number of electrodes, and the performance of the EEG amplifier can all in turn affect HEP topographies (Park and Blanke, 2019). As Park and Blanke (2019) identified, a systematic meta-analysis of HEP research is essential if HEP is to be utilised as a reliable, powerful and well-grounded indicator of cortical interoceptive processing of cardiac signals and to establish consistent processing methodologies to use HEP in clinical and research settings (Coll et al., 2021).

The aims of the review are threefold. Firstly, to better understand HEP processing methods used to date in the field in both EEG and MEG. This review aims to explore and quantify variability in the methodology and parameters used to record the heartbeat-evoked potential. Secondly, based on the HEP processing pipelines found in the literature, a sensitivity analysis will be performed to demonstrate the potential impact of different pipeline parameters on HEP values using EEG. Finally, this review aims to take an initial step towards fostering consensus about optimal and standardised HEP processing methods through an informed assessment of different methods to date and their impact on HEP signal.

2. Materials and methods

2.1. Scoping review search strategy

The literature search involved two electronic databases, Web of Science and PubMed, which yielded 1001 potential eligible studies. This was reduced to 124 studies (EEG and MEG studies) after removal of duplicates and exclusion of studies (figure 1). This search spanned from 1993 to 2023. A series of different combinations of key words were used for the literature search including Boolean operators (‘AND’ and ‘OR’) (table 1). The two studies using intracranial EEG (iEEG) were excluded as these were not significant.

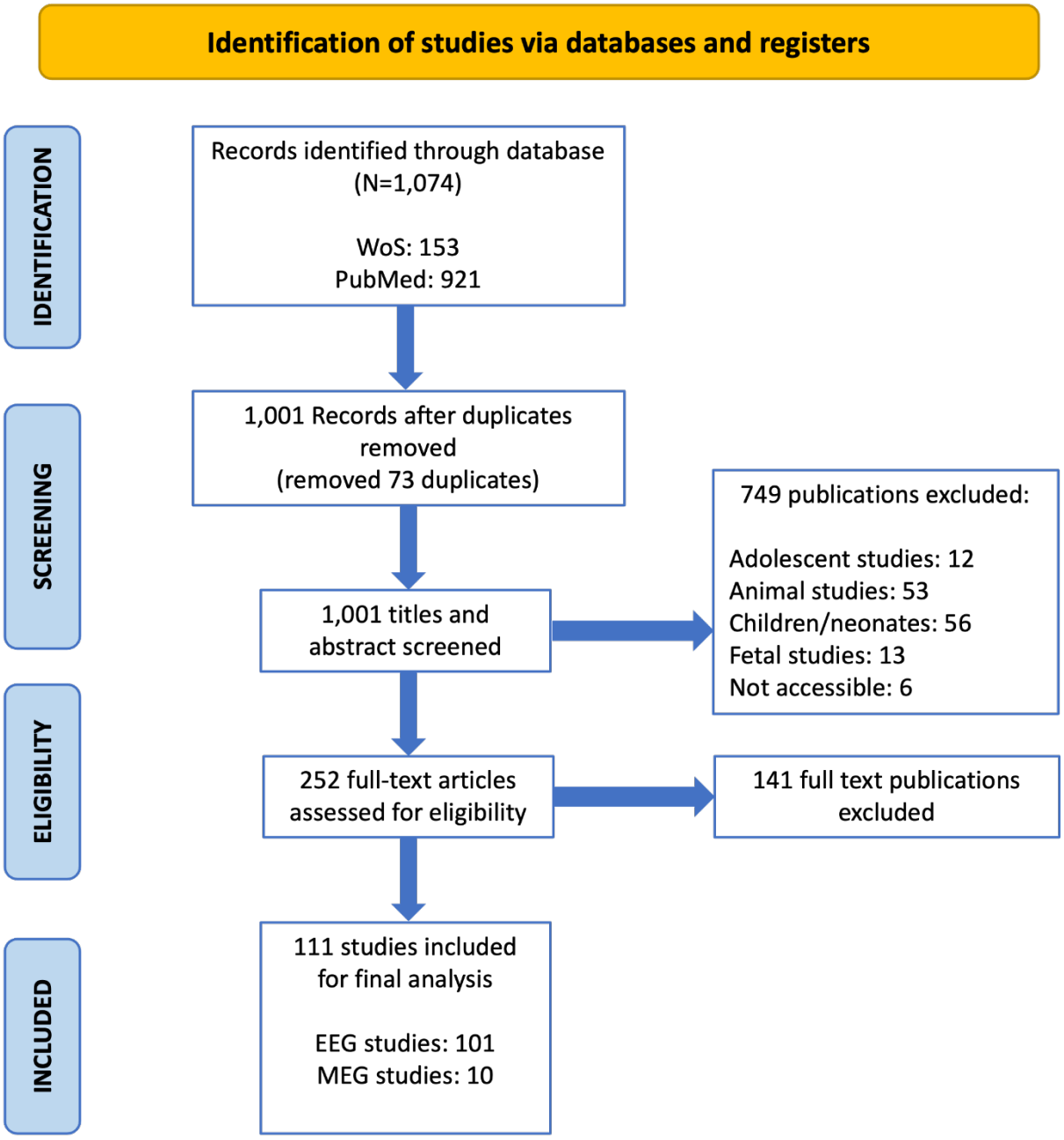

Figure 1. PRISMA flow diagram demonstrating the total number of publications included and removed at the different stages and the reasons for exclusion.

PubMed	Or	And
	"heart" or "heart rate"	"evoked potentials"
	"heart"	"evoked potential"
	"HEP"	"electroencephalography" or "electroencephalogram"
	"EEG" or "magnetoencephalography" or "magnetoencephalogram"	
	"MEG"	
Web of Science	"heartbeat evoked"	

Table 1. Search strategies used in different databases.

2.2. Inclusion and exclusion criteria

Inclusion criteria included specifically adult human HEP studies using EEG, MEG or iEEG. Exclusion criteria encompassed animal studies (rabbits, dogs, cats, rats), children and neonatal studies, adolescent studies, foetal studies, and other studies not related to HEP (such as other event-related potentials, epilepsy studies, viruses, or protein) or inaccessible studies.

2.3. Data collection and analysis

Full-text screening and data extraction was performed by the author and an independent reviewer (co-author: R.K.) flagged any inconsistencies during data extraction. Current processing techniques and parameters reported in the literature were examined. The data extracted from the studies underwent collation, synthesis, and analysis based on the following variables and their definitions (table 2, figure 2):

A. Low-pass and high-pass filter cut-off frequencies in Hertz (Hz)
B. Epoch timeframes in seconds (s)
C. Epoch relative to R wave or T wave
D. Epoch amplitude rejection in microvolts (μV)
E. HEP window in milliseconds (ms)
F. Baseline correction time frame in milliseconds (ms)
G. Minimum RR interval in milliseconds (ms)
H. CFA removal methodology
I. Electrodes used for EEG analysis

Following data extraction, statistical analysis was performed using Python version 3.9 and the MNE python package version 1.7.0.

Variable	Definition
Low-pass and high-pass cut-off frequencies (in Hz)	Artefact filter settings for initial bandpass processing. A low-pass filter allows low-frequency signals and blocks high-frequency signals, while a high-pass filter does the opposite.

Epoch timeframes in milliseconds (ms) (also referred to as epoch window)	Epochs are segments of data of equal lengths extracted from continuous EEG data.
Epoch relative to R wave or T wave	Epochs are typically centred around stimulus events or responses; here either to the R wave or T wave of the ECG.
Epoch amplitude rejection in microvolts (μV)	The scalp EEG amplitude recorded in any channel surpasses a predetermined threshold set in the study, resulting in the rejection of the epoch from further analysis because it is considered to be artifact.
HEP window in milliseconds (ms)	Latency range within which HEP is thought to be found – this varies between studies. Computation of the HEP at a specific lead involves computing the average baseline-corrected amplitude in this interval.
Baseline correction time frame in milliseconds (ms)	The baseline correction time frame in EEG is the time-period before stimulus onset. It serves to correct for any fluctuations or drifts in the EEG signal that could arise during recording, including movements, electrode drift, or alterations in brain activity.
Minimum RR interval in milliseconds (ms)	This is the shortest time-period between successive heartbeats that is considered for HEP analysis (the epochs associated with shorter RR intervals are excluded from analysis). The goal of this is to reduce the likelihood of the next heartbeat's associated electrical activity from interfering with the period of EEG used to derive the HEP.
Cardiac Field Artefact (CFA) removal methodology	Methodology used to remove cardiac field artifact such as independent component analysis (ICA), artefact subspace reconstruction (ASR), or Hjorth method.
Electrode used for EEG	These are the scalp electrodes used for EEG recording.

Table 2. Variables extracted from the literature and their definitions. Independent component analysis (ICA) is a signal processing technique which separates EEG signal into independent source components. Some of these components may correspond to artefacts such as muscle activity or eye movements. Artefact components are then identified, removed manually and computationally. Artefact subspace reconstruction (ASR) requires an initial calibration using segments (detected manually or automatically) of relatively clean baseline EEG data. ASR is designed to handle non-stationary/non-repeating artefacts using a sliding window and principal component analysis to identify and remove high-amplitude signal components. The three Hjorth parameters – activity (variance of the signal), mobility (mean frequency of the power spectrum), and complexity (estimation of the bandwidth of the signal) - are calculated

using time-domain signal processing approaches, which offer a statistical analysis of the signal's attributes. These parameters are used to identify and remove artefacts.

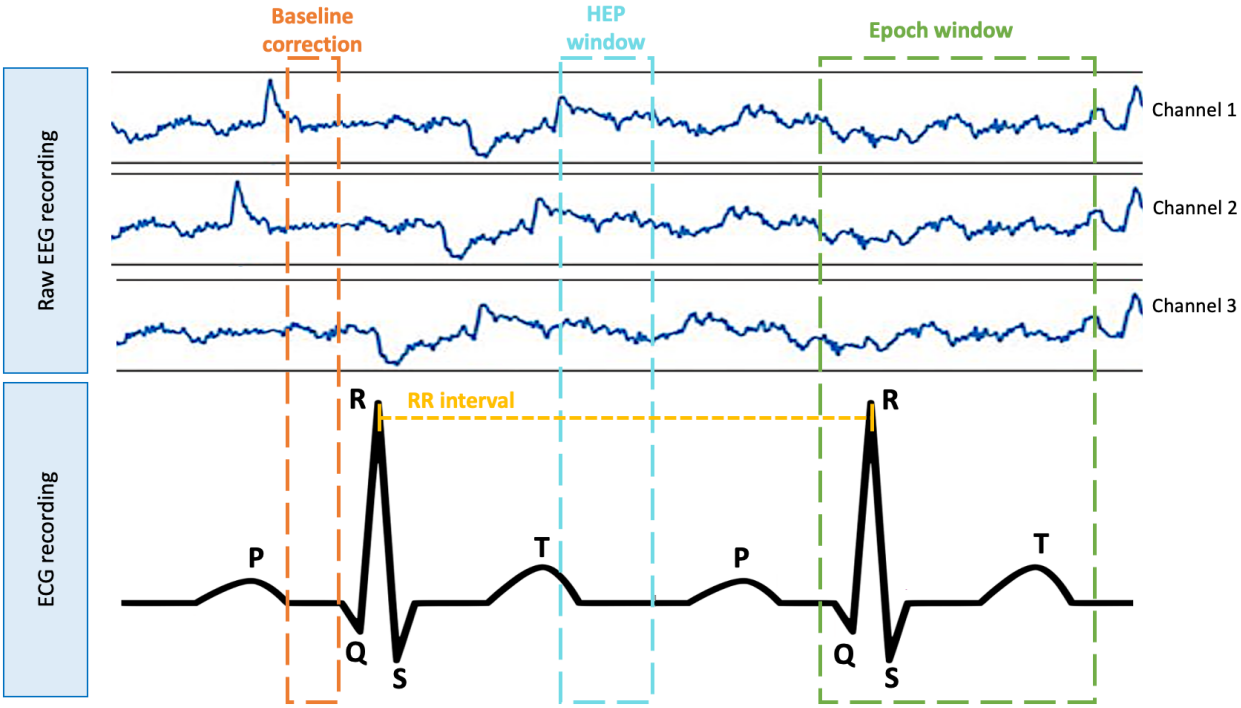

Figure 2. Diagram representing key elements of the EEG and ECG signals to process EEG and derive HEP. Note that the placement of the HEP window, epoch window and baseline correction window are prototypical and may vary in position relative to components on the ECG trace, depending on the study's methodology.

2.4. Processing pipeline methodology

The second part of this review aims to contribute to building consensus about optimal and standardised HEP processing methods through an informed assessment of different methods used to date in the literature and their impact on HEP signal. This was achieved by developing a signal processing pipeline for HEP. Different processing methods extracted from the literature were implemented and tested on available scalp EEG data (normal EEG studies from the Temple University EEG dataset (Obeid and Picone, 2016)) to explore how different methods and parameters affect the HEP extraction process and results. Factors explored for their effect on HEP included the same variables investigated during data extraction (section 2.3). To do this, relatively clean sections of EEG were clipped by hand (using EDFbrowser software version 1.4), then pre-processed with variable applications of artefact-subspace-reconstruction (ASR) or independent-component-analysis (ICA). Epochs were generated with various values of minimum RR threshold, maximum epoch amplitude, and filter settings (figure 3). HEP was then computed for each set of generated epochs. The variability of the HEP between epochs for a given set of parameters was analysed following the values described in Table 3 and in Figure 3. This was achieved for different pre-processing methods: ICA with CFA removed, ASR at different thresholds (5, 10, and 20) and uncorrected raw EEG (figure 3).

A sensitivity analysis was conducted to assess which variables have the greatest effect on HEP. For this, independent variables were varied (low-pass and high-pass for filtering settings, baseline start and baseline end for the baseline window, start of HEP window and end of HEP window for the HEP window, minimum RR interval and maximum epoch amplitude threshold) and the effect on dependent variables (HEP at Fp1, Fp2, Fz, Cz, Pz, F3, F4, F7, F8, C3, C4, P3, P4, T3, T4, T5, T6, O1, O2) was recorded in each filtering method (ASR 5, ASR 10, ASR 20, ICA with CFA removed, and uncorrected EEG). In a first instance, a Mann-Whitney U test was computed to compare the effect of each filtering method on the number of epochs exceeding amplitude threshold. This was followed a one-way ANOVA, performed on the data to determine which independent variables derived from the literature significantly affected the derived HEP values at the aforementioned EEG leads (figure 3).

High pass (in Hz)	Low pass (in Hz)	Maximum epoch amplitude (in µV)	Minimum RR interval (in seconds)
0.01	15	30	0.5
0.05	20	50	0.55
0.1	24	70	0.6
0.3	24	75	0.65
0.5	**30**	80	0.7
0.7	35	**100**	0.75
1	40	120	0.8
-	45	150	**0.88**
-	50	250	0.9
-	62.5	300	-
-	80	-	-
-	100	-	-

Table 3. Snapshot of values for the pre-processing variables extracted from the literature review. These were used to compute the HEP in the analysis. Values in bold were identified as the modal values in the literature (complete list of values and details in Figure 3).

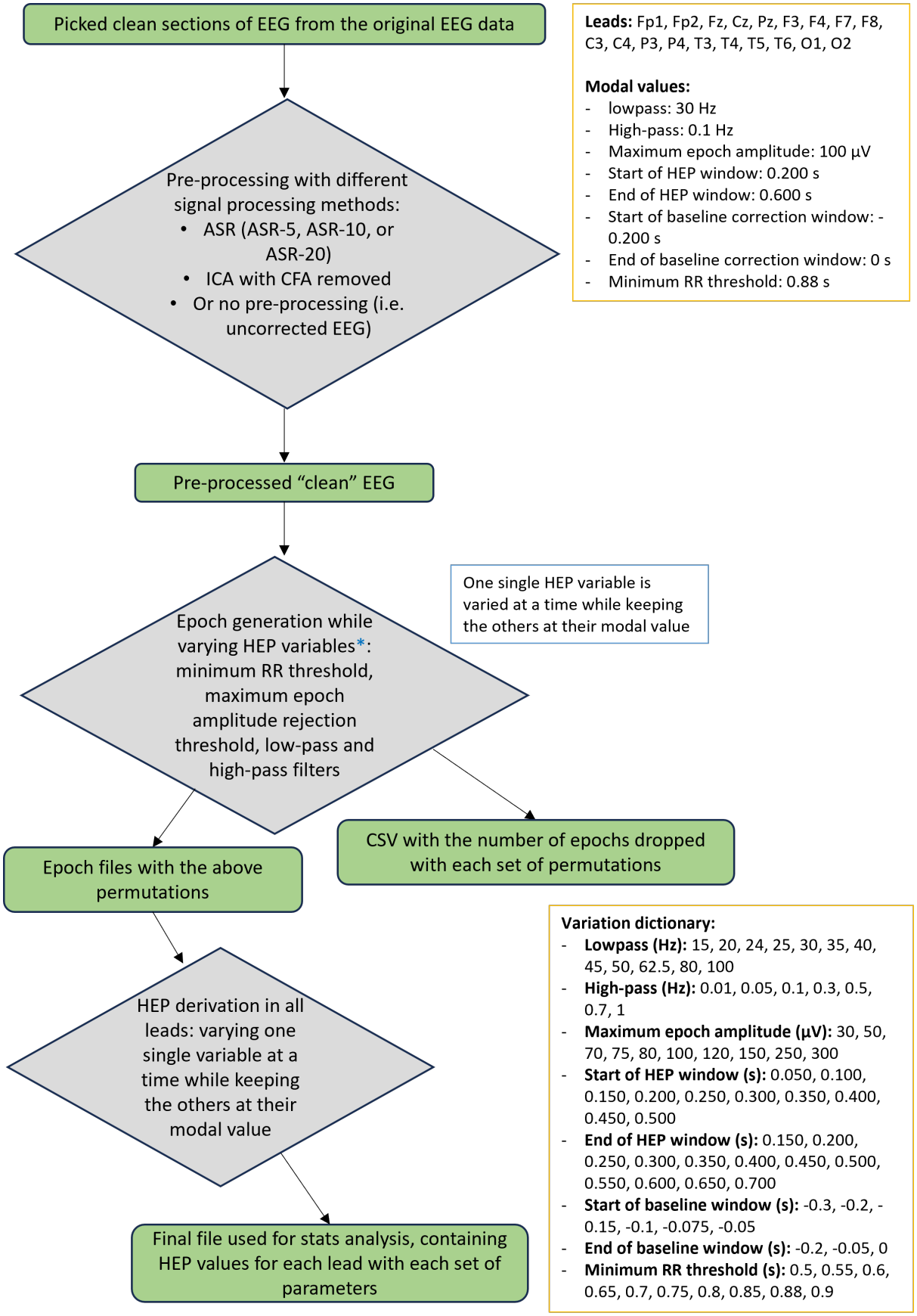

Figure 3: Flowchart illustrating the data processing methodology with values used for analysis and HEP computation and EEG channels considered. CSV – comma separated value files.

2.5. Artefact Correction methods

EEG is comprised of electrical potentials originating from various sources (Ungureanu et al., 2004). Artefacts from physiological sources (cardiac field artefact, pulse artefact, myogenic artefact) and non-physiological sources (electrode pops, movement) generate electrical activity that contaminate this EEG data. ICA and ASR are two distinct source-separation methods. These are effective techniques that are widely used to remove signal components related to non-brain activity and improve the signal quality of EEG (Plechawska-Wójcik et al., 2023). ICA and ASR were applied iteratively on the EEG data to subsequently compare their effect on artefact removal and HEP signal derivation.

2.5.1. Independent component analysis

ICA seeks to find and disentangle statistically independent components that are linearly mixed across multiple sensors. Data is assumed to be non-gaussian. During signal processing, ICA coefficients are computed and are used to determine that spatial contribution on the signal component (Aljobouri, 2023; Carvalho, 2023). Components that appear artefactual are identified and removed, and the EEG signal is then reconstructed without the artefact (Ungureanu et al., 2004). ICA may require some initial manual intervention to categorise components as artefactual or EEG. In this review, ICA was applied using functions from MNE, and then artefactual components were identified using mne-icalabel, and the ICA then fitted to the original EEG signal, at the pre-processing stage after picking clean sections of EEG from the original EEG data (figure 3) (Li et al., 2022).

2.5.2. Artefact Subspace Reconstruction

ASR is a newer and more automated method which models and removes subspaces created by artefacts. The ASR process can be divided into three steps (Chang et al., 2019). First, reference data is extracted with ASR automatically detecting clean segments of raw EEG data based on the distribution of signal variance (Chang et al., 2019). The second step involves establishing thresholds for determining artefact components. Lastly, it eliminates artefact components and reconstructs cleaned data. One of the most important user-defined parameters in ASR is the cut-off parameter denoted as '*k'* (Chang et al., 2019). This parameter delineates the rejection thresholds in units of standard deviation, i.e. '*k'* is the parameter of the ASR algorithm regulating the threshold above which components would be identified as artifacts. Chang et al. (2019) demonstrated that the value of 'k' affects the performance of ASR for removing artefacts. The present study employed k values of 5, 10, and 20. In our analysis we applied ASR using the ASRpy package, an implementation of ASR in the python programming language.

3. Results

3.1. Literature scoping review – gaps and inconsistencies in HEP processing methods

Analysis of the HEP literature using the variables detailed previously, demonstrated a high level of heterogeneity in terms of the measures reported when deriving HEP in both EEG and MEG studies (table 4, table 5). These results highlighted the lack of consistency in reporting variables used for HEP derivation. The variables the least reported by the literature in EEG studies were the epoch amplitude rejection threshold (80.2%), the number of samples (epochs) used for analysis (92%) and the minimum RR interval (97%) (table 4). Similar results were noted for MEG results where no studies reported on the epoch amplitude rejection value, and the number of samples used for analysis (table 5).

Unreported variables	Number of studies	Percentage (%)
Low-pass and/or high-pass filters	25	24.75
Epoch window	5	4.95
Epochs relative to the R wave or T wave	3	2.97
Epoch amplitude rejection threshold (μV)	81	80.2
HEP windows	16	15.84
Number of samples used for analysis	93	92.08
Baseline correction	52	51.49
Minimum RR interval	98	97.03
CFA correction	38	37.62
Electrodes used unreported	28	27.72

Table 4. The number of studies and the corresponding percentage where variables were unreported based on the 101 extracted EEG studies.

Unreported variables	Number of studies	Percentage (%)
Low-pass and high-pass filters	2	20
Epoch window	1	10
Epochs relative to the R wave or T wave	3	30
Epoch amplitude rejection threshold (μV)	10	100
HEP windows	6	60
Number of samples used for analysis	10	100
Baseline correction	9	90
Minimum RR interval	9	90
CFA correction	1	10

Table 5. The number of studies and the corresponding percentage where variables were unreported based on the 10 extracted MEG studies.

3.2. Literature scoping review – heterogeneity in HEP parameter values

The literature demonstrated a significant level of heterogeneity in the values used for each parameter for HEP derivation (figure 4). Modal values may support the development of consensus values for HEP computation (table 6). Indeed, 26 studies used 30 Hz as the low-pass filter cut-off frequency (A) with a range from 15 Hz to 100 Hz. The two most common (modal values) high-pass cut-off frequencies (B) were 0.1 Hz and 0.5 Hz, used in 26 studies. Fifty-two studies applied an epoch start time (C) at -200 ms and 49 studies utilised 600 ms as the epoch end time (D), in relation to the reference point utilised in the paper (R or T wave or unspecified). Two hundred milliseconds was identified as the modal value for the start of the HEP window (E) across 33 studies. These studies showed an overall spread ranging from 0 ms to 550 ms, measured in relation to the R wave. Studies using the T wave as a reference point or those that were unspecified were excluded as these represented 4 of the total number of studies processed. Thirty-four studies employed 600 ms as the end of the HEP window (F) with values starting from 150 ms to 700 ms. Twenty-six studies used -200 ms for the start of the baseline correction window (G) with a range from -300 ms to 200 ms. For 44 studies, 0 ms was the modal value for the end time of the baseline correction (H). Lastly, 5 studies used 50 μV as the epoch amplitude rejection threshold (I) with another 5 studies employing 100 μV as the threshold. The range of values spread from 30 μV to 300 μV.

HEP variable	Modal value	Number of studies
Low-pass filter	30 Hz	26
High-pass filter	**0.1 Hz**	26
High-pass filter	0.5 Hz	26
Epoch window start time	-200 ms	52
Epoch window end time	600 ms	49
Start of the HEP window	200 ms	33
End of the HEP window	600 ms	34
Start of baseline correction window	-200 ms	26
End of baseline correction window	0 ms	44
Epoch amplitude rejection threshold	50 μV	5
Epoch amplitude rejection threshold	**100 μV**	5

Table 6: Modal values identified in the literature and the number of studies employing these values. Values in bold indicate the chosen modal value for that HEP variable.

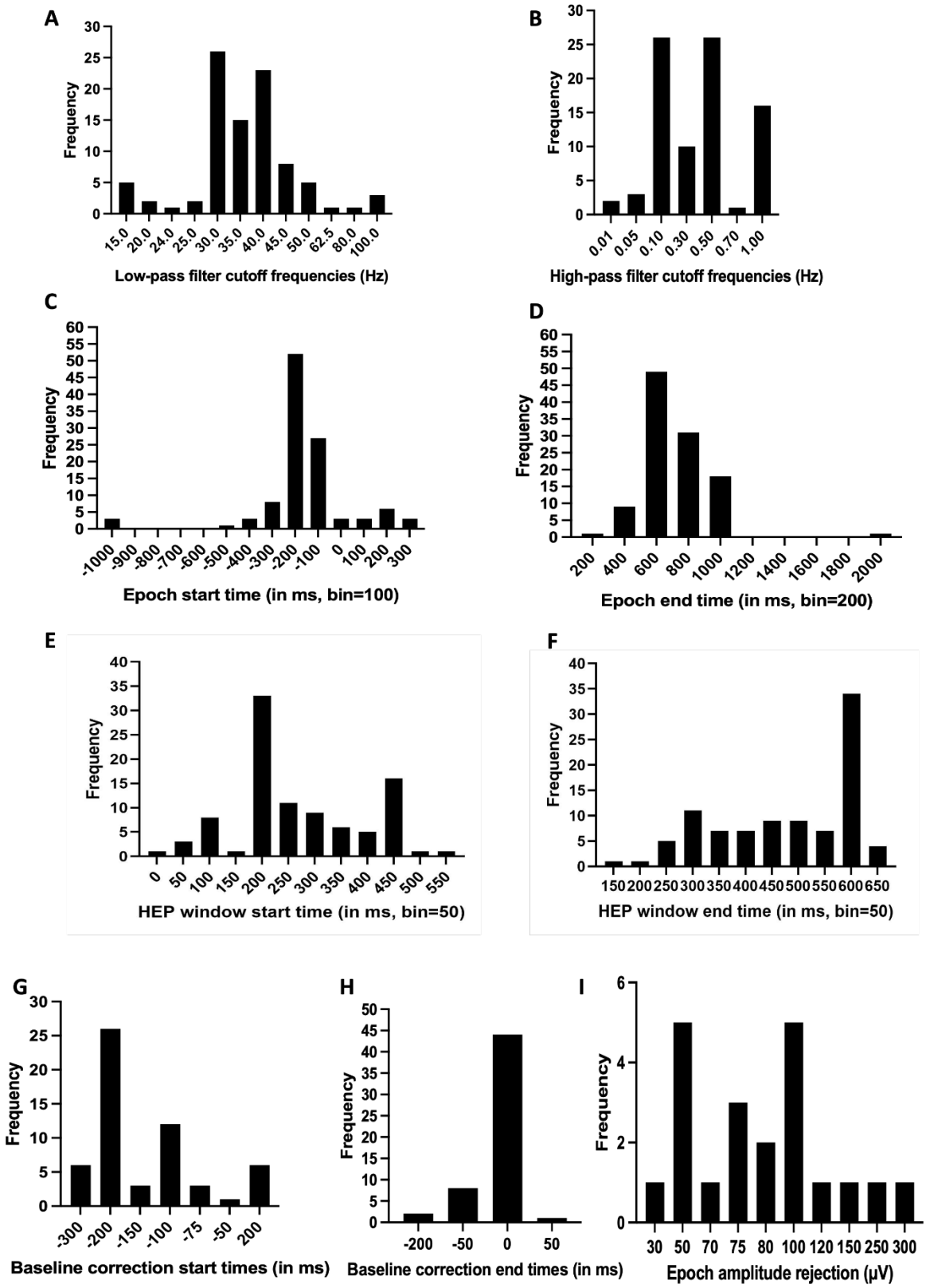

Figure 4. Values obtained from the literature used for each parameter (low pass (A) and high pass (B) filter cut-off frequencies, epoch start time (C) and end time (D), HEP window start time (E) and end time (F), baseline correction start time (G) and end time (H), epoch amplitude rejection (I) to derive HEP.

3.3. Sensitivity analysis of HEP processing parameters

To assess the impact of each processing parameter (minimum RR, start and end times of the HEP window and start and end times of the baseline correction window) involved in deriving HEP, EEG data was epoched according to different parameter values extracted from the literature (figure 3). Figure 5 describes the relation between the number of epochs (in percentage) below the minimum RR threshold. As the RR interval increased, more epochs were dropped for further analysis as they do not meet the RR threshold, i.e. those epochs were too short. Epochs where the time until the next R wave was less than the minimum RR threshold may increase the risk of CFA affecting the HEP. Figure 6 describes the relation between the percentage of epochs exceeding the amplitude threshold and the epoch amplitude rejection threshold. The percentage of epochs excluded decreased rapidly when the maximum epoch amplitude was below 100 μV, after which it remained relatively constant at 40 epochs (5%) exceeding the amplitude threshold. When the amplitude threshold is varied, there is a clear threshold effect; amplitudes below 100 μV lead to an exponential increase in the number of epochs rejected. Conversely, above 100 μV, there is little change in the number of epochs rejected. In wakefullness, EEG is mostly under 100 μV. Therefore, there is not a significant change in the number of epochs exceeding the amplitude rejection threshold passed 100 μV. Figure 7 represents the number of epochs exceeding amplitude threshold following the application of the different filtering techniques identified in the literature (ASR 5, ASR 10, ASR 20, ICA with CFA removed and uncorrected EEG) using the modal values defined for high pass filters (0.1 Hz), low pass filters (30 Hz), maximum epoch amplitude rejection (100 μV) and minimum RR interval (0.88 s). Overall, ASR-5, ASR-10, ASR-20 and ICA with CFA removed seem to yield similar results in terms of the reduction in epochs exceeding the amplitude threshold.

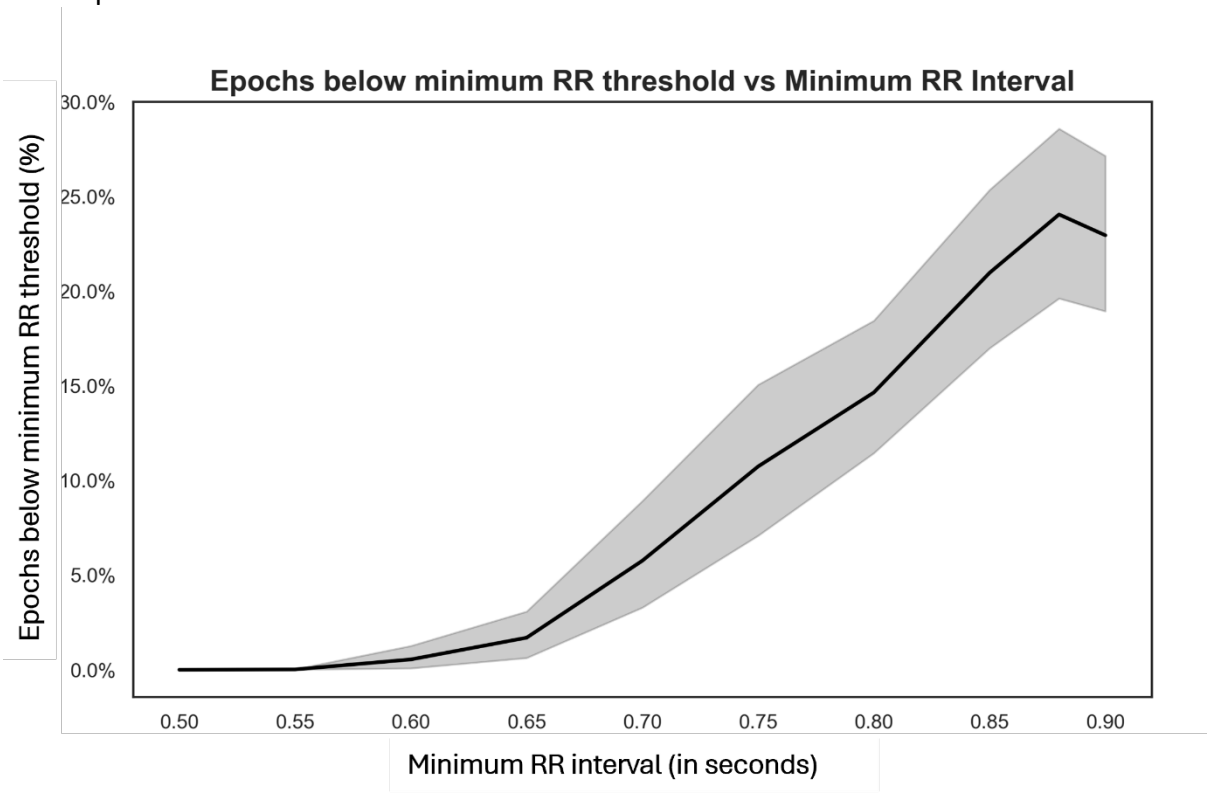

Figure 5. The number of epochs (represented in %) below minimum RR threshold according to the minimum RR interval (in milliseconds) across all filtering methods (ICA, ASR, and uncorrected EEG).

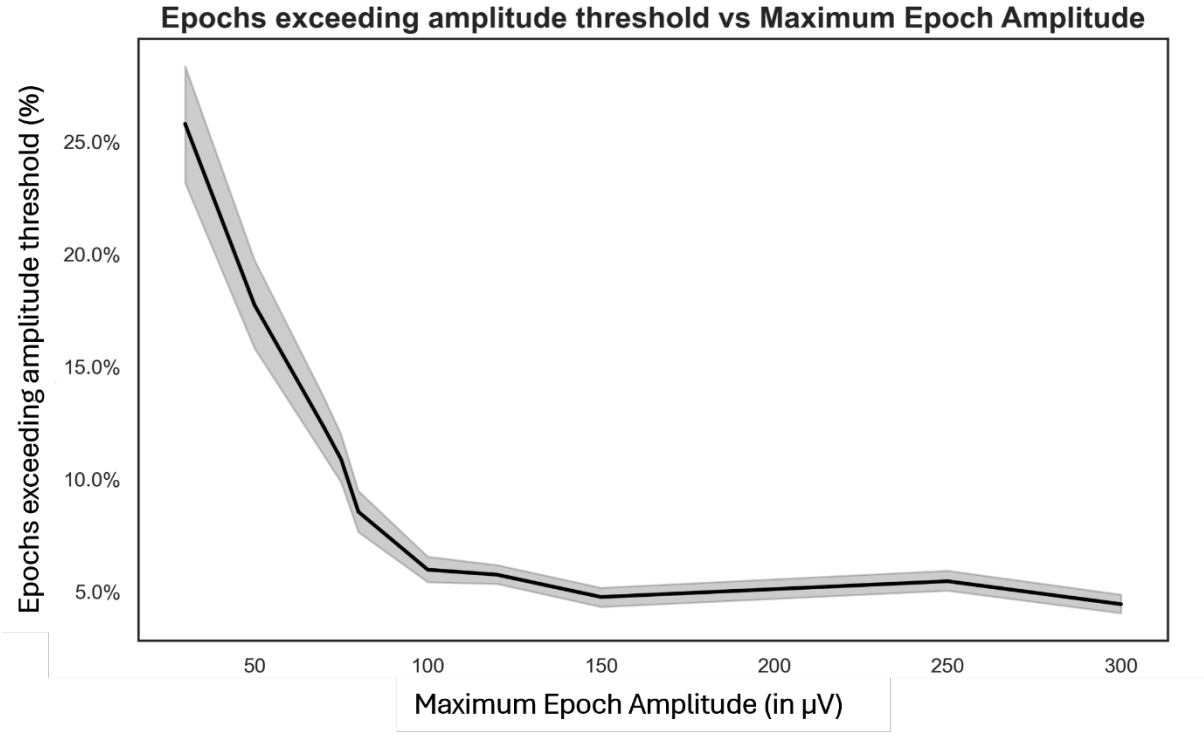

Figure 6. The number of epochs (represented in %) with too much artefact according to the maximum epoch amplitude (in µV) across all filtering methods (ICA, ASR, and uncorrected EEG).

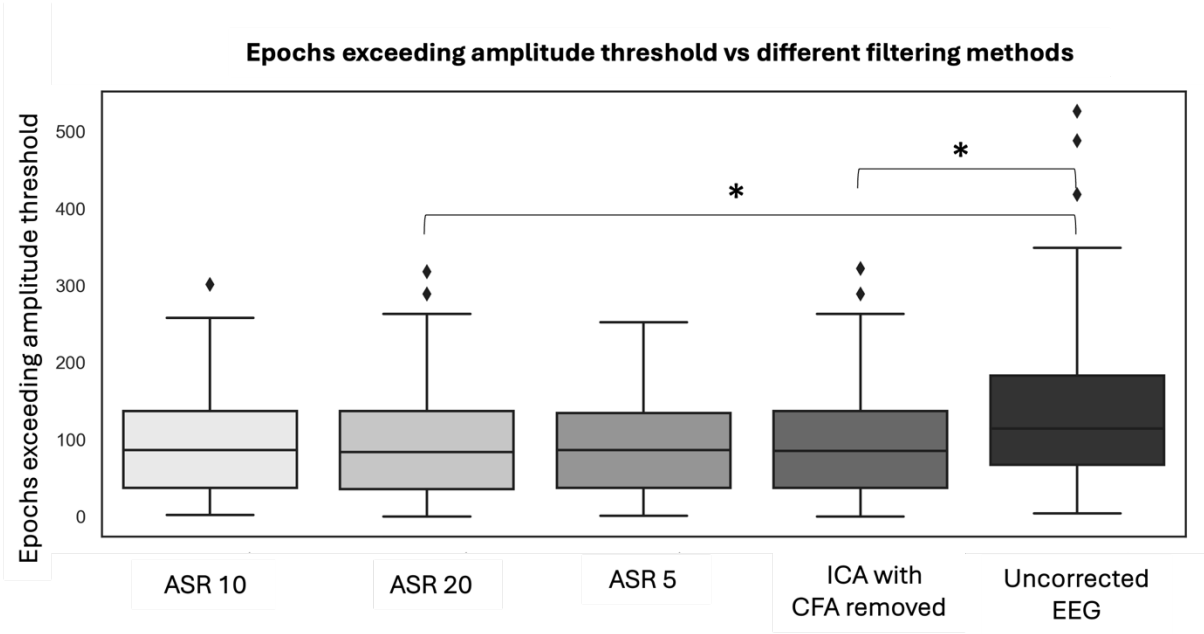

Figure 7. Box plot representing the number of epochs exceeding the amplitude threshold in relation to the different filtering parameters using the modal values defined for high pass

filters (0.1 Hz), low pass filters (30 Hz), epoch amplitude rejection (100 μV) and minimum RR interval (0.88 seconds).

Figure 8 depicts the grand averages of EEG evoked potentials as voltage maps. This analysis was conducted to increase signal-to-noise ratio and reveal evoked potential morphology across different filtering methods. Each point on the voltage map represents the instanteneous voltage at that lead. Panel A represents grand averages of uncorrected EEG data which is noisy as expected. The concentration of signals in the time series of panel B (ICA with CFA removed) suggests that the ICA with CFA removal method could have effectively removed artefacts and noise. Panel E with a less aggressive ASR threshold of 20, seems to exhibit a similar signal to ICA with CFA removed. Grand averages in panel D with a more constraining ASR threshold (ASR-10) seem to contain more oscillations than other panels (i.e. ASR-5). These oscillations could be due to low variance being in synchrony with the heartbeats. Observations are further supported with statistical analysis in 3.4.3.

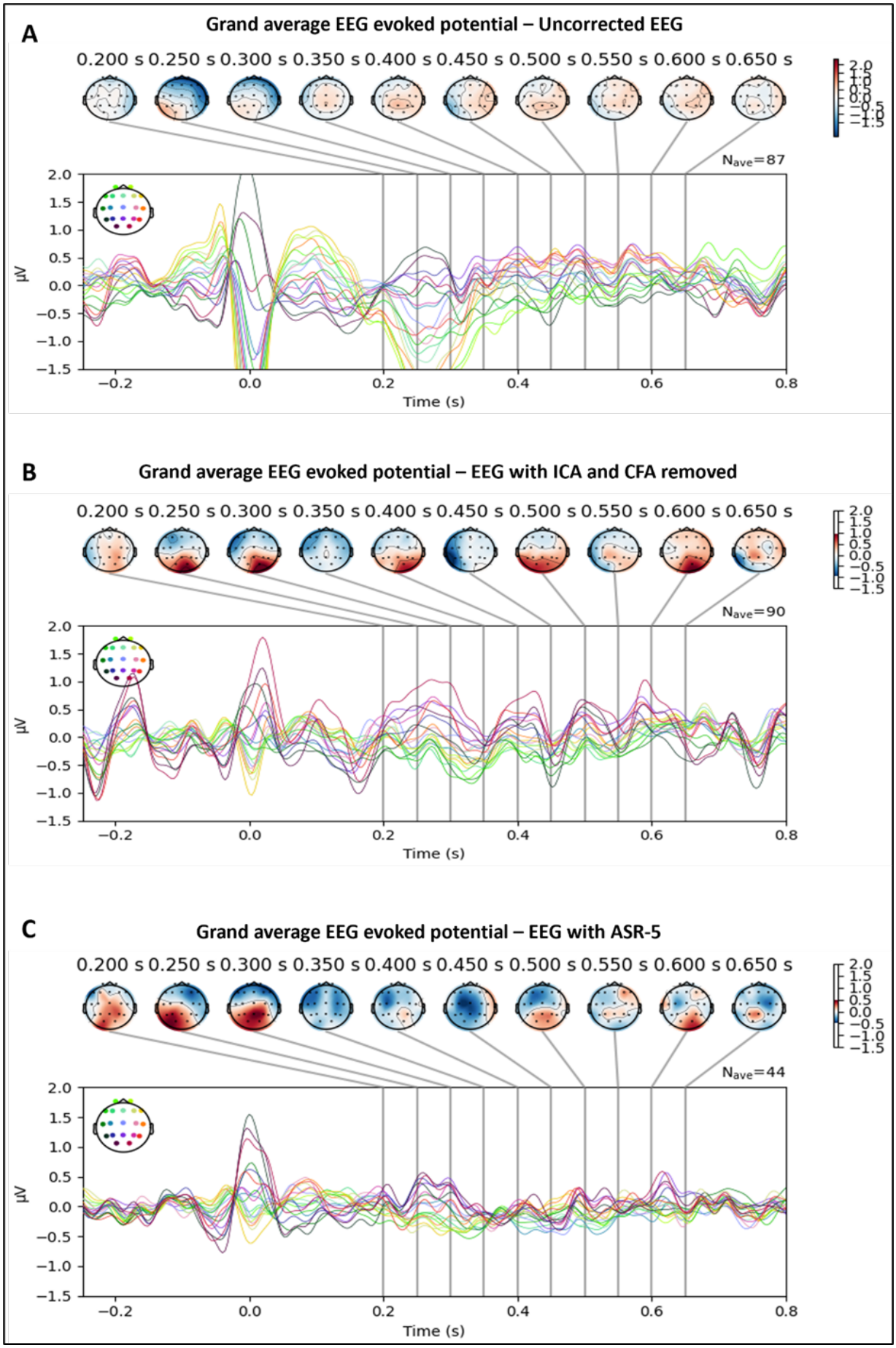
A
Grand average EEG evoked potential – Uncorrected EEG
0.200 s 0.250 s 0.300 s 0.350 s 0.400 s 0.450 s 0.500 s 0.550 s 0.600 s 0.650 s
Nave=87
µV
Time (s)
B
Grand average EEG evoked potential – EEG with ICA and CFA removed
0.200 s 0.250 s 0.300 s 0.350 s 0.400 s 0.450 s 0.500 s 0.550 s 0.600 s 0.650 s
Nave=90
µV
Time (s)
C
Grand average EEG evoked potential – EEG with ASR-5
0.200 s 0.250 s 0.300 s 0.350 s 0.400 s 0.450 s 0.500 s 0.550 s 0.600 s 0.650 s
Nave=44
µV
Time (s)

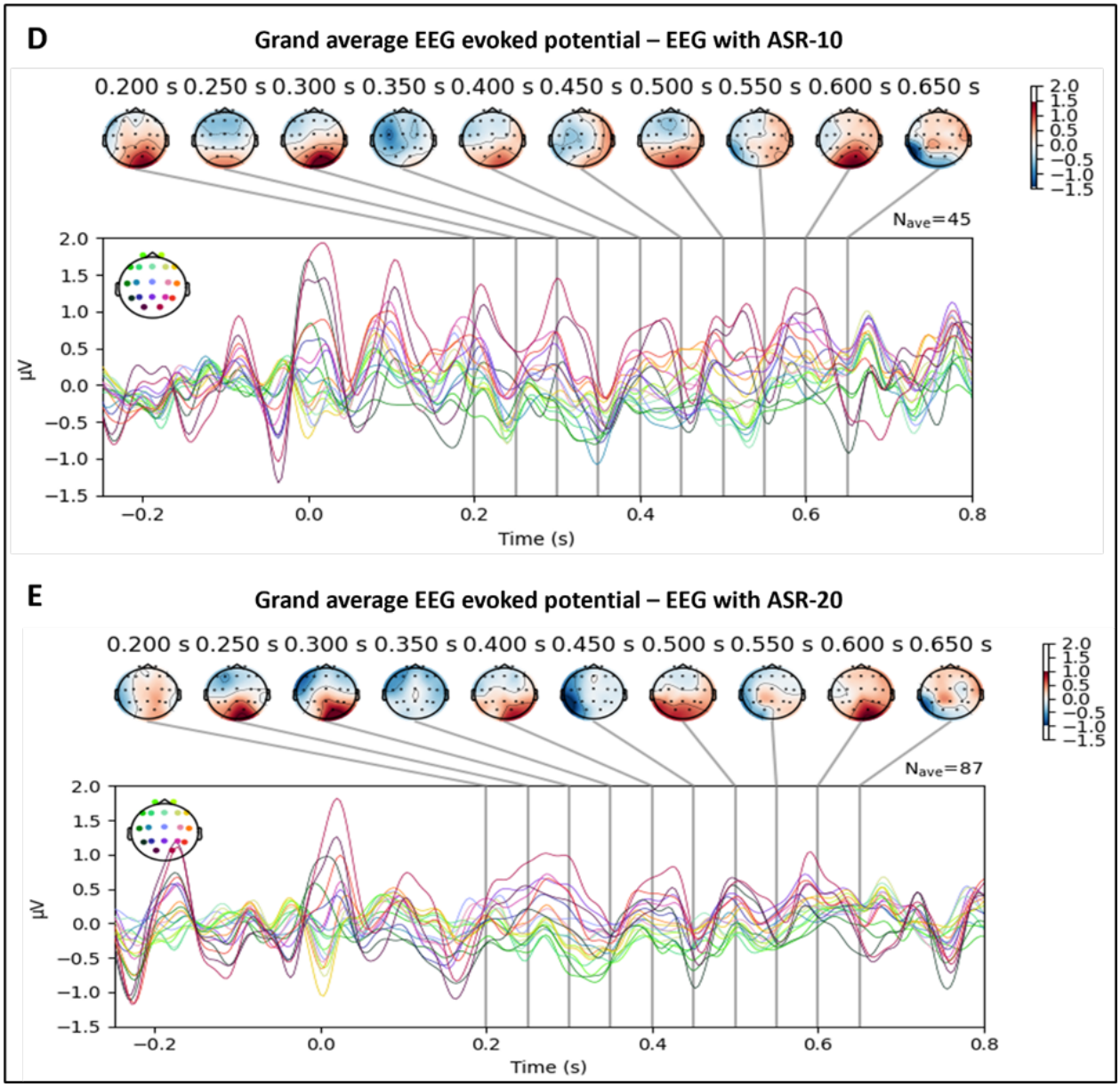

Figure 8. Grand average topographical voltage maps across filtering methods.

3.4. Sensitivity analysis: Mann-Whitney U test and ANOVA analysis – modal value investigation

3.4.1. Mann-Whitney U test – effect of filtering methods on the number of epochs exceeding maximum epoch amplitude threshold

A Mann-Whitney U test (independent samples T-test) was conducted to assess the effect of different EEG filtering methods on the number of epochs exceeding the maximum epoch amplitude threshold (figure 7, figure 9). This non-parametric statistical test was chosen as the data was non-normal. After Bonferroni correction, α was set at 0.01. While there was no significant difference between the different artefact correction methods, there was a significant difference between the artefact correction methods and uncorrected EEG,

particularly between ASR-20 and uncorrected EEG (p<0.001) and ICA with CFA removed and uncorrected EEG (p=0.002) after Bonferroni correction which supports the results in figure 7 and figure 8.

	ASR-5	**ASR-10**	**ASR-20**	**ICA with CFA removed**	**Uncorrected EEG**
ASR-5					
ASR-10	U=1230.500p =0.834				
ASR-20	U=2261.500p =0.862	U=2382.500 p=0.737			
ICA with CFA removed	U=2363.000p =0.957	U=2400.500 p=0.922	U=4444.000 p=0.764		
Uncorrected EEG	U=1755.000p =0.010	U=1782.000 p=0.014	U=3285.500 p<.001*	U=3488.000 p=0.002*	

Figure 9: Matrix representation of Mann-Whitney U test. Results illustrate the effect of the filtering methods explored on the number of epochs exceeding the maximum epoch amplitude threshold. Bonferroni correction was set at α = 0.01. All other variables were kept at their modal values (high pass filter – 0.1 Hz, low pass filter – 30 Hz, epoch amplitude rejection – 100 μV, minimum RR interval – 0.88 seconds).

3.4.2. ANOVA results for HEP variables in ICA with CFA removed

To produce a more accurate analysis, the ANOVA analysis was conducted by considering filtering method and variables investigated. Statistical analysis was performed in JASP (version 0.18.3.0). This was followed by Bonferroni correction to reduce the risk of type I errors. Parametric variables were modified one at a time, with the remaining values at their modal value from the literature. This was performed in ICA with CFA removed only, as ICA is the most used method in the literature for signal processing and was therefore considered as the "modal" filtering method. The number of epochs dropped at each iteration was used as weights in the statistical analysis in JASP to prevent confounding. Results (table 7) demonstrated that HEP is significantly affected in the central electrodes when considering the start of the baseline correction window (in ms) (F(5, 5870) = 3.443, p=0.004* at C3), the start of the HEP window (in ms) (F(9, 5866) = 2.360, p=0.012* at C3) and the end of the HEP window (in ms) (F(9, 5866) = 3.485, p<.001** at Cz and F(9, 5866) = 3.414, p<.001** at C3). HEP seems to also be affected in temporal channels when looking at the start of the baseline correction window (in ms) (F(5, 5870) = 4.507,p<.001** at T5), and the minimum RR (in ms) (F(9, 5866) = 3.553, p<.001** at T6). Although significance was not present after Bonferroni correction (α = 0.0026), HEP is also affected in pre-frontal (Fp1) and frontal (F3) electrodes when considering the minimum RR (in ms) (F(9, 5866) = 2.587, p=0.006* in Fp1 and F(9, 5866) =

2.685, p=0.004* in F3). Low pass and high pass values were also varied as defined in figure 3, but the different parametric values did not significantly affect HEP.

Channels	F statistic and P-value
Start of the Baseline Correction Window (ms)	
C3	F(5, 5870) = 3.443, p=0.004*
T5	F(5, 5870) = 4.507, p<.001**
Start of the HEP Window (ms)	
C3	F(9, 5866) = 2.360, p=0.012*
End of the HEP Window (ms)	
Cz	F(9, 5866) = 3.485, p<.001**
C3	F(9, 5866) = 3.414, p<.001**
O2	F(9, 5866) = 2.352, p=0.012*
Minimum RR (ms)	
Fp1	F(9, 5866) = 2.587, p=0.006*
F3	F(9, 5866) = 2.685, p=0.004*
T6	F(9, 5866) = 3.553, p<.001**
O1	F(9, 5866) = 2.014, p=0.034*
O2	F(9, 5866) = 5.597, p<.001**

Table 7. ANOVA results conducted for modal values of HEP variables in ICA with CFA removed. Bonferroni correction at α = 0.0026. Asterisks represent significance before (* - significance before Bonferroni correction) and after Bonferroni correction (** - significance after Bonferroni correction). Low pass and high pass filters had no effect on HEP amplitude and results were not significant.

3.4.3. ANOVA results for HEP variables in different artefact settings

The second part of the ANOVA analysis examined the effect of different artefact processing methods (ICA versus ASR) on HEP amplitude in different channels (table 8). The results indicate no significance between ICA and ASR-20 in any channel. Significant effects are seen in both ICA versus ASR-5 and ICA versus ASR-10 in all channels after Bonferroni correction (α = 0.0026) except for P4 and T6 in ICA versus ASR-5 and in F3 and T3 in ICA versus ASR-10.

EEG Channels	ICA with CFA removed vs ASR-5	ICA with CFA removed vs ASR-10	ICA with CFA removed vs ASR-20
	F statistic and P value (α = 0.0026)		
Fp1	F(1, 7507) = 5.458, p=0.020	F(1, 7523) = 2.682, p=0.102	F(1, 9892) = 0.011, p=0.915
Fp2	F(1, 7507) = 75.635, p<.001**	F(1, 7523) = 69.994, p<.001**	F(1, 9892) = 1.425, p=0.233
Fz	F(1, 7507) = 49.441, p<.001**	F(1, 7523) = 48.053, p<.001**	F(1, 9892) = 1.115, p=0.291

Cz	F(1, 7507) = 33.566, p<.001**	F(1, 7523) = 42.347, p<.001**	F(1, 9892) = 0.687, p=0.407
Pz	F(1, 7507) = 0.082, p=0.775	F(1, 7523) = 0.170, p=0.680	F(1, 9892) = 0.001, p=0.972
F3	F(1, 7507) = 27.933, p<.001**	F(1, 7523) = 8.689, p=0.003	F(1, 9892) = 0.003, p=0.959
F4	F(1, 7507) = 61.319, p<.001**	F(1, 7523) = 45.245, p<.001**	F(1, 9892) = 1.129, p=0.288
F7	F(1, 7507) = 47.598, p<.001**	F(1, 7523) = 48.657, p<.001**	F(1, 9892) = 0.064, p=0.801
F8	F(1, 7507) = 44.861, p<.001**	F(1, 7523) = 27.491, p<.001**	F(1, 9892) = 0.056, p=0.813
C3	F(1, 7507) = 20.238, p<.001**	F(1, 7523) = 14.876, p<.001**	F(1, 9892) = 2.668x10^(-4), p=0.987
C4	F(1, 7507) = 0.233, p=0.629	F(1, 7523) = 1.033, p=0.310	F(1, 9892) = 0.059, p=0.808
P4	F(1, 7507) = 6.937, p=0.008	F(1, 7523) = 0.055, p=0.814	F(1, 9892) = 0.111, p=0.739
T3	F(1, 7507) = 0.809, p=0.368	F(1, 7523) = 8.437, p=0.004	F(1, 9892) = 0.024, p=0.878
T4	F(1, 7507) = 21.037, p<.001**	F(1, 7523) = 26.028, p<.001**	F(1, 9892) = 0.007, p=0.935
O1	F(1, 7507) = 94.667, p<.001**	F(1, 7523) = 35.736, p<.001**	F(1, 9892) = 0.426, p=0.514
O2	F(1, 7507) = 29.482, p<.001**	F(1, 7523) = 0.255, p=0.614	F(1, 9892) = 0.258, p=0.612

Table 8. Results of the ANOVA conducted for modal values of HEP variables in ICA with CFA removed versus ASR. Bonferroni correction at α = 0.0026. F statistics and p-values in bold represent significance after Bonferroni. The asterisks represent significance before (* - significance before Bonferroni correction) and after Bonferroni correction (** - significance after Bonferroni correction).

Table 9 represents the effect of ICA with CFA removed or ASR and uncorrected EEG on HEP in different channels. HEP seems to be significantly affected by signal processing methods in most channels despite Bonferroni correction at α = 0.0026.

EEG Channels	**ICA with CFA removed vs uncorrected EEG**	**ASR-5 vs uncorrected EEG**	**ASR-10 vs uncorrected EEG**	**ASR-20 vs uncorrected EEG**
	F statistic and P-value			
Fp1	F(1, 9937)=4.844, p=0.028*	F(1, 7386)=0.163, p=0.686	F(1, 7402)=13.147, p<.001**	F(1, 9771)=5.285, p=0.022**

Fp2	F(1, 9937)=1057.185, p<.001**	F(1, 7386)=1126.673, p <.001**	F(1, 7402)=1080.307, p<.001**	F(1, 9771)=1111.839, p<.001**
Fz	F(1, 9937)=1419.927, p <.001**	F(1, 7386)=1357.669, p<.001**	F(1, 7402)=1313.194, p <.001**	F(1, 9771)=1473.351, p <.001**
Cz	F(1, 9937)=122.125, p <.001**	F(1, 7386)=211.956,p <.001**	F(1, 7402)=222.282, p <.001**	F(1, 9771)=139.998, p <.001**
Pz	F(1, 9937)=8.517, p=0.004*	F(1, 7386)=4.362,p =0.037*	F(1, 7402)=6.900, p=0.009*	F(1, 9771)=8.313, p=0.004*
F3	F(1, 9937)=2.065, p=0.151	F(1, 7386)=43.431,p <.001**	F(1, 7402)=17.388, p<.001**	F(1, 9771)=1.904, p=0.168
F4	F(1, 9937)=114.378, p<.001**	F(1, 7386)=245.687,p <.001**	F(1, 7402)=213.206, p<.001**	F(1, 9771)=134.005, p <.001**
F7	F(1, 9937)=194.994, p<.001**	F(1, 7386)=279.459,p <.001**	F(1, 7402)=276.142, p <.001**	F(1, 9771)=197.212, p <.001**
F8	F(1, 9937)=132.763, p <.001**	F(1, 7386)=259.232,p <.001**	F(1, 7402)= 208.924, p <.001**	F(1, 9771)=135.473, p <.001**
C3	F(1, 9937)=122.211, p <.001**	F(1, 7386)=169.440,p <.001**	F(1, 7402)= 151.157, p <.001**	F(1, 9771)=120.021, p <.001**
P4	F(1, 9937)=6.789, p=0.009*	F(1, 7386)=22.399,p <.001**	F(1, 7402)= 5.767, p =0.016**	F(1, 9771)=5.256, p=0.022*
T3	F(1, 9937)=9.413, p 0.002**	F(1, 7386)=11.592,p <.001**	F(1, 7402)= 0.115, p =0.735	F(1, 9771)=10.386, p=0.001**
T4	F(1, 9937)=33.357, p<.001**	F(1, 7386)=90.233,p <.001**	F(1, 7402)= 95.869, p <.001**	F(1, 9771)=33.176, p<.001**
T5	F(1, 9937)=4.037, p 0.045*	F(1, 7386)=0.128,p=0.721	F(1, 7402)= 0.473, p =0.492	F(1, 9771)=2.993, p=0.084
T6	F(1, 9937)=26.660, p<.001**	F(1, 7386)=3.719,p=0.054	F(1, 7402)= 26.526, p <.001**	F(1, 9771)=28.496, p <.001**
O1	F(1, 9937)=1.616, p=0.204	F(1, 7386)=103.110,p <.001**	F(1, 7402)= 44.045, p <.001**	F(1, 9771)=3.526, p=0.060*

O2	F(1, 9937)=20.383, p<.001**	F(1, 7386)=0.672,p =0.412	F(1, 7402)= 10.258, p=0.001**	F(1, 9771)=24.627, p<.001**

Table 9. ANOVA results conducted for modal values of HEP variables in ICA with CFA removed versus ASR. Bonferroni correction at α = 0.0026. The asterisk represent significance before (* - significance before Bonferroni correction) and after Bonferroni correction (** - significance after Bonferroni correction).

Table 10 demonstrates the effect of different levels of ASR artefact removal settings on HEP in different channels. HEP seems to be less affected in ASR-10 and ASR-5 than in ASR-20 despite Bonferroni correction α = 0.0026.

EEG Channels	ASR-10 vs ASR-5	ASR-10 vs ASR-20	ASR-5 vs ASR-20
	F statistic and P-value		
Fp1	F(1, 4972)=22.018, p <.001**	F(1, 7357)=2.408, p =0.121	F(1, 7341)=5.970, p =0.015**
Fp2	F(1, 4972)=0.010, p=0.920	F(1, 7357)=55.108, p<.001**	F(1, 7341)=59.909, p <.001**
Fz	F(1, 4972)=0.026, p=0.873	F(1, 7357)=37.043, p<.001**	F(1, 7341)=38.066, p <.001**
Cz	F(1, 4972)=1.569, p=0.210	F(1, 7357)=35.304, p<.001**	F(1, 7341)=27.013, p <.001**
Pz	F(1, 4972)=0.401, p=0.527	F(1, 7357)=0.197, p=0.657	F(1, 7341)=0.068, p=0.795
F3	F(1, 4972)=4.244, p=0.039	F(1, 7357)=8.946, p=0.003*	F(1, 7341)=28.466, p <.001**
F4	F(1, 4972)=1.820, p=0.177	F(1, 7357)=34.274, p<.001**	F(1, 7341)=48.362, p <.001**
F7	F(1, 4972)=0.144, p=0.705	F(1, 7357)=45.915, p<.001**	F(1, 7341)=44.891, p <.001**
F8	F(1, 4972)=2.590, p=0.108	F(1, 7357)=25.382, p<.001**	F(1, 7341)=42.164, p <.001**
C3	F(1, 4972)=0.396, p=0.529	F(1, 7357)=0.693, p=0.405	F(1, 7341)=20.063, p<.001**
P4	F(1, 4972)=6.817, p=0.009*	F(1, 7357)=0.271, p=0.603	F(1, 7341)=8.811, p= 0.003*
T3	F(1, 4972)=12.616, p <.001**	F(1, 7357)=9.383, p=0.002**	F(1, 7341)=0.615, p= 0.433

T4	F(1, 4972)=0.895, p=0.344	F(1, 7357)=24.588, p<.001**	F(1, 7341)=19.789, p<.001**
T5	F(1, 4972)=0.387, p=0.534	F(1, 7357)=0.968, p=0.325	F(1, 7341)=2.383, p=0.123
T6	F(1, 4972)=18.939, p <.001**	F(1, 7357)=0.283, p=0.595	F(1, 7341)=9.055, p=0.003*
O1	F(1, 4972)=13.537, p <.001**	F(1, 7357)=29.904, p<.001**	F(1, 7341)=85.326, p <.001**
O2	F(1, 4972)=27.239, p <.001**	F(1, 7357)=0.882, p=0.348	F(1, 7341)=35.846, p<.001**

Table 10. ANOVA results conducted for modal values of HEP variables at different levels of ASR artefact removal settings. Bonferroni correction at α = 0.0026. the asterisk represent significance before (* - significance before Bonferroni correction) and after Bonferroni correction (** - significance after Bonferroni correction).

4. Discussion

Results from the literature scoping review demonstrated a significant level of heterogeneity in the values used for HEP derivation and lack of consistency in terms of variables reported in studies. This demonstrates the fundamental need for a processing pipeline to derive HEP to ensure replicability and consensus in this growing field.

As expected, increasing the allowed RR interval increases the number of epochs that meet the criteria (figure 5). Epochs shorter than the minimum RR threshold could cause the infiltration of cardiac field artefacts which would impact HEP computation and may lead to inaccurate results. Epochs containing activity with amplitudes exceeding the amplitude threshold value are thought likely to do so due to artefact, rather than EEG activity, and higher amplitudes are more likely to skew averaged evoked responses (figure 6). Investigating the impact of filtering methods on the number of epochs exceeding amplitude threshold, demonstrated that all filtering methods remove epochs with large amplitude artefacts from EEG data (figure 7). P-values were not significant after Bonferroni correction for ASR-5 and ASR-10 versus uncorrected EEG. However, ASR-20 and ICA with CFA removed showed significant results for removing artefact from EEG in comparison to uncorrected EEG (figure 9).

Topographies of the evoked EEG potentials (figure 8) and the corresponding statistical analysis (table 8-10) demonstrated that filtering methods significantly affect HEP in specific EEG channels. As expected, ICA and ASR seem to clearly affect HEP versus uncorrected EEG (table 8), which is important as signal processing is essential for the accurate computation of any evoked potential. Overall, ASR-5 and ASR-10 do not strongly affect the amplitude of HEP. However, ASR-20 significantly affects HEP across most channels, confirming ASR's efficacy as a signal-preprocessing method. In addition, it seems the signal processing methods using ASR-20 and ICA with CFA removed lead to fewer epochs remaining, which exceed the amplitude

threshold (figure 9). This may suggest that ASR using a *'k'* value threshold of 20 is as performant as ICA with CFA removed (table 8, figure 8). Indeed, Plechawska-Wójcik et al. (2023) suggested the optimal ASR parameter to be between 20 and 30. However, a delicate balance must be struck to remove artefacts efficiently without removing or aberrantly altering the EEG signal. Overall, this is an exciting finding as ICA has been predominantly used in the literature until now. Given that ASR can be utilised concurrently with EEG acquisition, its potential application in future wearable technologies might be possible.

ANOVA analysis (table 7) using modal values demonstrated that the RR interval, the start and end of the HEP window and the start of the baseline correction window significantly affect HEP in certain channels as described earlier. These broadly correspond to the pre-frontal, frontal and centrotemporal electrodes which are suggested to be some of the more fruitful regions for extracting HEP at the scalp (F3, Fp1, C3, and Cz) (Park and Blanke, 2019). The RR interval represents the interval in which HEP is found and comprises of one heartbeat. The minimum RR is therefore the smallest interval in which a single HEP amplitude can be found. If this interval is too short, there is a greater risk that the HEP value derived would be contaminated by the CFA, which can be an order of magnitude greater than the HEP signal. Given this significant effect, it is concerning that 97% of EEG studies do not report either whether a minimum RR interval has been used and, if so, at what value. The RR interval should be carefully considered during EEG analysis. HEP derivation in participants with tachycardia is at risk of finding an inflated HEP value. The start and end of the HEP window are critical for deriving HEP and minimising contamination by the CFA. As demonstrated by the scoping review, about 16% of studies do not report on this value, which underpins the HEP analysis. Similarly, approximately 52% of studies do not explicitly state the baseline correction window, which this review has demonstrated to affect the HEP. As investigated, CFA correction is crucial for a reliable HEP value. The literature revealed that ≈38% of studies do not report whether CFA correction was performed or not. Specific electrodes seem to affect HEP more than others, yet ≈28% of studies do not report on the electrodes used for analysis. These results highlight the indisputable lack of consistency within the field. Hence, particular care should be given to these variables when acquiring and deriving HEP to ensure consistency and standardisation of analysis.

5. Conclusion

The present study suggests that the RR interval, the start and end of the HEP window and the start of the baseline correction window significantly affect HEP in specific channels as described. These channels appear to broadly align with the pre-frontal, frontal, and centrotemporal electrodes, which are thought to be particularly involved areas for extracting HEP from the scalp. Some of these effects disappear after Bonferroni correction, indicating that while there is a potential tendency for these variables to affect HEP outcome and should be treated with caution during analysis, their effects should be further investigated. Critical values for reliable HEP extraction should be reported in publications, emphasising the need for standardised methods to enhance study comparison and reproducibility and establish a gold standard in the field. However, these findings are based on one EEG dataset, and whether these effects would be observed in other EEG acquisition setups is unknown. The scoping review investigated the lack of consistency in MEG data, but analysis was only conducted for

EEG data. Future work should examine how HEP is affected by the use of windows relative to the T wave rather than the R wave. In addition, as there is no "ground truth" for HEP, this review has aimed to investigate how HEP extraction parameters influence and affect the resulting HEP. Ultimately, to develop robust methods for HEP derivation, it is essential to establish a "ground truth" for HEP with a clear consensus on CFA removal. Such standardisation would provide a reliable foundation for advancing research and enhancing the accuracy of HEP. This review serves as a basis for further work in this matter.

Data and Code Availability: the code is publicly available on GitHub at https://github.com/RaniaImanV/HEP-PARAMs.git.

Author contributions: All authors were involved in the conceptualisation, methodology, the review and editing of the drafts and supervision (M.Y., S.N.G., D.C.). R.I.V. and R.K. were involved in the investigation, software development (primarily R.K.), and formal analysis. R.I.V. created the visualisation and wrote the original draft.

Funding: M.Y. is funded by an MRC CARP award (MR/V037676/1).
R.I.V. - This work was supported by the Biotechnology and Biological Sciences Research Council [grant number BB/T008709/1]

Declaration of competing interests: the authors attest to no competing interests.

Ethics statement: this study did not involve testing on humans or animals.

References:

Aljobouri, H. K. (2023). Independent component analysis with functional neuroscience data analysis. *Journal of Biomedical Physics & Engineering, 13*(2), 169–180. https://doi.org/10.31661/jbpe.v0i0.2111-143

Arnau, S., Sharifian, F., Wascher, E., & Larra, M. F. (2023). Removing the cardiac field artifact from the EEG using neural network regression. *Psychophysiology, 60*(10). https://doi.org/10.1111/psyp.14323

Babo-Rebelo, M., Richter, C. G., & Tallon-Baudry, C. (2016a). Neural responses to heartbeats in the default network encode the self in spontaneous thoughts. *Journal of Neuroscience, 36*(29), 7829–7840.

Baranauskas, M., Grabauskaitė, A., & Griškova-Bulanova, I. (2017). Brain responses and self-reported indices of interoception: Heartbeat evoked potentials are inversely associated with worrying about body sensations. *Physiology & Behavior, 180*, 1–7. https://doi.org/10.1016/j.physbeh.2017.07.032

Canales-Johnson, A., Silva, C., Huepe, D., Rivera-Rei, A., Noreika, V., Garcia, M. D., Silva, W., Ciraolo, C., Vaucheret, E., Sedeno, L., Couto, B., Kargieman, L., Baglivo, F., Sigman, M.,

Chennu, S., Ibanez, A., Rodriguez, E., & Bekinschtein, T. A. (2015). Auditory feedback differentially modulates behavioral and neural markers of objective and subjective performance when tapping to your heartbeat. *Cerebral Cortex, 25*(12), 4490–4503.

Chang, C.-Y., Hsu, S.-H., Pion-Tonachini, L., & Jung, T.-P. (2019). Evaluation of artifact subspace reconstruction for automatic artifact components removal in multi-channel EEG recordings. *IEEE Transactions on Biomedical Engineering*, 1–1. https://doi.org/10.1109/tbme.2019.2930186

Coll, M.-P., Hobson, H., Bird, G., & Murphy, J. (2021). Systematic review and meta-analysis of the relationship between the heartbeat-evoked potential and interoception. *Neuroscience & Biobehavioral Reviews, 122*, 190–200. https://doi.org/10.1016/j.neubiorev.2020.12.012

Flasbeck, V., Popkirov, S., Ebert, A., & Brüne, M. (2020). Altered interoception in patients with borderline personality disorder: A study using heartbeat-evoked potentials. *Borderline Personality Disorder and Emotion Dysregulation, 7*(1). https://doi.org/10.1186/s40479-020-00139-1

Garfinkel, S. N., & Critchley, H. D. (2016). Threat and the body: How the heart supports fear processing. *Trends in Cognitive Sciences, 20*(1), 34–46. https://doi.org/10.1016/j.tics.2015.10.005

Gray, M. A., Taggart, P., Sutton, P. M., Groves, D., Holdright, D. R., Bradbury, D., Brull, D., & Critchley, H. D. (2007). A cortical potential reflecting cardiac function. *Proceedings of the National Academy of Sciences, 104*(16), 6818–6823. https://doi.org/10.1073/pnas.0609509104

Jones, G. E., Leonberger, T. F., Rouse, C. H., Caldwell, J. A., & Jones, K. R. (1986). Preliminary data exploring the presence of an evoked potential associated with cardiac visceral activity. *Psychophysiology, 23*, 445.

Kamp, S.-M., Schulz, A., Forester, G., & Domes, G. (2021). Older adults show a higher heartbeat-evoked potential than young adults and a negative association with everyday metacognition. *Brain Research, 147238*. https://doi.org/10.1016/j.brainres.2020.147238

Kern, M., Ad Aertsen, Schulze-Bonhage, A., & Ball, T. (2013). Heart cycle-related effects on event-related potentials, spectral power changes, and connectivity patterns in the human ECoG. *NeuroImage, 81*, 178–190. https://doi.org/10.1016/j.neuroimage.2013.05.042

Khalsa, S. S., Adolphs, R., Cameron, O. G., Critchley, H. D., Davenport, P. W., Feinstein, J. S., Feusner, J. D., Garfinkel, S. N., Lane, R. D., Mehling, W. E., Meuret, A. E., Nemeroff, C. B., Oppenheimer, S., Petzschner, F. H., Pollatos, O., Rhudy, J. L., Schramm, L. P., Simmons, W. K., Stein, M. B., & Stephan, K. E. (2018). Interoception and mental health: A roadmap. *Biological Psychiatry: Cognitive Neuroscience and Neuroimaging, 3*(6), 501–513. https://doi.org/10.1016/j.bpsc.2017.12.004

Khalsa, S. S., Rudrauf, D., Feinstein, J. S., & Tranel, D. (2009). The pathways of interoceptive awareness. *Nature Neuroscience, 12*(12), 1494–1496. https://doi.org/10.1038/nn.2411

Kim, K. J., Ramiro Diaz, J., Iddings, J. A., & Filosa, J. A. (2016). Vasculo-neuronal coupling: Retrograde vascular communication to brain neurons. *Journal of Neuroscience, 36*(47), 12624–12639.

Kumral, D., Al, E., Cesnaite, E., Kornej, J., Sander, C., Hensch, T., Zeynalova, S., Tautenhahn, S., Hagendorf, A., Laufs, U., Wachter, R., Nikulin, V., & Villringer, A. (2022). Attenuation of the heartbeat-evoked potential in patients with atrial fibrillation. *JACC: Clinical Electrophysiology, 8*(10), 1219–1230. https://doi.org/10.1016/j.jacep.2022.06.019

Maister, L., Tang, T., & Tsakiris, M. (2017). Neurobehavioral evidence of interoceptive sensitivity in early infancy. *eLife, 6*. https://doi.org/10.7554/elife.25318

Obeid, I., & Picone, J. (2016). The Temple University Hospital EEG data corpus. *Scholarshare*. https://doi.org/10.34944/dspace/5136

Pang, J., Tang, X., Li, H., Hu, Q., Cui, H., Zhang, L., Li, W., Zhu, Z., Wang, J., & Li, C. (2019). Altered interoceptive processing in generalized anxiety disorder: A heartbeat-evoked potential research. *Frontiers in Psychiatry, 10*. https://doi.org/10.3389/fpsyt.2019.00616

Park, H.-D., & Blanke, O. (2019). Heartbeat-evoked cortical responses: Underlying mechanisms, functional roles, and methodological considerations. *NeuroImage, 197*, 502–511. https://doi.org/10.1016/j.neuroimage.2019.04.081

Plechawska-Wójcik, M., Augustynowicz, P., Kaczorowska, M., Zabielska-Mendyk, E., & Zapała, D. (2023). The influence assessment of artifact subspace reconstruction on the EEG signal characteristics. *Applied Sciences, 13*(3), 1605. https://doi.org/10.3390/app13031605

Pollatos, O., & Schandry, R. (2004). Accuracy of heartbeat perception is reflected in the amplitude of the heartbeat-evoked brain potential. *Psychophysiology, 41*(3), 476–482. https://doi.org/10.1111/1469-8986.2004.00170.x

Pollatos, O., Herbert, B. M., Mai, S., & Kammer, T. (2016). Changes in interoceptive processes following brain stimulation. *Philosophical Transactions of the Royal Society B: Biological Sciences, 371*(1708). https://doi.org/10.1098/rstb.2016.0016

Elkommos, S., Martín-López, D., Koreki, A., Jolliffe, C., Kandasamy, R., Mula, M., Critchley, H. D., Edwards, M., Garfinkel, S. N., Richardson, M., & Yogarajah, M. (2023). Changes in the heartbeat-evoked potential are associated with functional seizures. *Journal of Neurology, Neurosurgery, and Psychiatry, 94*(9), 769–775. https://doi.org/10.1136/jnnp-2022-330167

Elkommos, S., Martín-López, D., Koreki, A., Jolliffe, C., Mula, M., Critchley, H. D., Edwards, M. J., Garfinkel, S. N., Richardson, M., & Yogarajah, M. (2022). Attenuated heart-brain

integration predicts functional non-epileptic seizures. *Journal of Neurology, Neurosurgery, and Psychiatry, 93*(12), e3.7–e3.7. https://doi.org/10.1136/jnnp-2022-bnpa.15

Shamsaei, N., Shen, K. R., Wilder-Smith, E., Ong, C. J., & Li, X. (2010). Heartbeat evoked potential: A neural correlate of pain perception? *Proceedings of the 32nd Annual International Conference of the IEEE Engineering in Medicine and Biology Society (EMBC)*, 1578–1581. https://doi.org/10.1007/978-3-642-14515-5_402

Schandry, R., Sparrer, B., & Weitkunat, R. (1986). From the heart to the brain: A study of heartbeat contingent scalp potentials. *International Journal of Neuroscience, 30*, 261-275.

Schmitz, M., Müller, L. E., Seitz, K. I., Schulz, A., Steinmann, S., Herpertz, S. C., & Bertsch, K. (2021). Heartbeat evoked potentials in patients with post-traumatic stress disorder: An unaltered neurobiological regulation system? *European Journal of Psychotraumatology, 12*(1). https://doi.org/10.1080/20008198.2021.1987686

Suksasilp, C., & Garfinkel, S. N. (2022). Towards a comprehensive assessment of interoception in a multi-dimensional framework. *Biological Psychology, 168*, 108262. https://doi.org/10.1016/j.biopsycho.2022.108262

Tahsili-Fahadan, P., & Geocadin, R. G. (2017). Heart–brain axis. *Circulation Research, 120*(3), 559–572. https://doi.org/10.1161/circresaha.116.308446

Terhaar, J., Viola, F. C., Bär, K.-J., & Debener, S. (2012). Heartbeat evoked potentials mirror altered body perception in depressed patients. *Clinical Neurophysiology, 123*(10), 1950–1957. https://doi.org/10.1016/j.clinph.2012.02.086

Ungureanu, M., Bigan, C., Strungaru, R., & Lazarescu, V. (2004). Independent component analysis applied in biomedical signal processing. *Measurement Science Review, 4*(2).

Yuan, H., Yan, H.-M., Xu, X.-G., Han, F., & Yan, Q. (2007). Effect of heartbeat perception on heartbeat evoked potential waves. *Neuroscience Bulletin, 23*(6), 357–362. https://doi.org/10.1007/s12264-007-0053-7